A CROSS-CORRELATION MODEL FOR NON-ISOTROPIC SCATTERING WITH NON-OMNIDIRECTIONAL ANTENNAS IN MIMO PROPAGATION CHANNELS

Hamidreza Saligheh Rad and Saeed Gazor

Department of Electrical and Computer Engineering
Queen's University, Kingston, Ontario, K7L 3N6, Canada.
Tel: (613) 533-6591, Fax: (613) 533-6615, Email: radh,gazors@ee.queensu.ca

ABSTRACT

We present a cross-correlation model for Multiple-Input Multiple-Output (MIMO) Rayleigh fading channels in a two-dimensional (2D) multipath random media when energy is non-uniformly received/transmitted to/from the receiver/transmitter along propagation directions. We investigate the impact of non-omnidirectional propagation pattern of antennas along with the impact of non-uniform distribution of the scatterers in the propagation environment which introduces non-isotropic wave propagation, at both transmitter and receiver ends. The non-isotropic propagation is described by non-uniform probability density functions (pdf) for the direction-of-departure (DOD) and the direction-of-arrival (DOA) of the outgoing/incoming propagating waves from/to stations. The propagation patterns of antenna elements (and the effect of mutual coupling between them) are also described by the Fourier series expansion of antenna propagation patterns. The expression of the cross-correlation function (CCF) turns out to be a linear expansion of a number of Bessel functions of the first kind. The coefficients of this expansion are given by linear convolution of the Fourier series coefficients (FSC) of the corresponding antenna patterns and the FSCs of the corresponding pdf of the non-isotropic propagation directions. The Fourier analysis on the CCF shows impacts of non-isotropic environment and non-omnidirectional antennas on the spectrum of the received channel process while the maximum Doppler frequency shift remains invariant with variations of beam-patterns and the pdf of propagating waves.

1. INTRODUCTION

Multiple-Input Multiple-Output (MIMO) communication system is a promising solution for wireless applications. The accurate and simple space-time-frequency (STF) wave propagation models have a major role to efficiently design a MIMO wireless system and to study its performance [1]. An approach to characterize MIMO channels is to analyze the statistical behavior of the time-varying STF channel transfer function (TF) in terms of physical parameters of the random scattering media. In this approach, the channel TF is represented by a sum of propagating waves over a number of paths. In each path, the signal reaches the receiver with a response described by the pdfs of some random variables. These random variables are phase, delay, direction-of-departure (DOD) and direction-of-arrival (DOA). In order to describe a non-isotropic propagation media, most of existing MIMO channel models assume a power density distribution either for the received energy or for the received waveform of the propagating paths. This distribution is known as power azimuth spectrum (PAS) or azimuth angular spread (AAS) for the distribution of the energy or the waveform, respectively. In the literature, these distributions are justified using experimental results [2–4]. Martin in [2] suggests a Laplacian (double-sided exponential) pdf for the relative DOA of the first multipath component, i.e., for the line-of-sight, and a zero-mean truncated Gaussian pdf for the relative DOA variables associated with other paths. Pedersen, Mogensen and Fleury find that in typical urban environments, PAS is accurately described by a Laplacian function, while a Gaussian function matches the shape of the AAS [3]. Abdi, Barger and Kaveh propose the use of the versatile von-Mises angular distribution for modeling the nonuniform AAS at the mobile station (MS) [4].

Here we calculate the cross-correlation function (CCF) of the MIMO channel TF versus different time-indices and carrier frequencies. We characterize the non-isotropic scattering environment by the Fourier Series Coefficients (FSCs) of the pdf of the propagating directions distribution. We also consider the effect of the antenna patterns (and the mutual coupling between array elements) by the Fourier series expansions (FSE) of the antenna propagation patterns (APP). Consequently, the CCF turns out to be a linear combination of the Bessel functions of the first kind. The coefficients of this linear combination are given by the convolution of the FSEs of the pdfs of both AASs and APPs.

The rest of this paper is organized as follows: Notations and assumptions are introduced in Section 2. The space-time-frequency CCF is derived in Section 3 by considering the effect of the non-isotropic wave propagation and the effect of the APPs. Conclusions and discussions are summarized in Section 4.

0-7803-8867-4/05/$20.00©2005 IEEE

Table 1. Non-Isotropic AAS and Corresponding FSCs

pdf, $f_\theta(\theta), \forall\theta \in [-\pi, \pi)$		FSCs, $\mathcal{F}_k$
Truncated Normal:	$\frac{\exp\left(-\frac{\theta^2}{2a^2}\right)}{\mathrm{erf}\left(\frac{\pi}{\sqrt{2}a}\right)\sqrt{2\pi}a}$	$\frac{\mathrm{Re}\left\{\mathrm{erf}\left(\frac{\pi+jka^2}{\sqrt{2}a}\right)\right\}}{\mathrm{erf}\left(\frac{\pi}{\sqrt{2}a}\right)} e^{-\frac{k^2a^2}{2}}$
Truncated Laplace:	$\frac{\exp\left(-\frac{\lvert\theta\rvert}{a}\right)}{2a\left(1-e^{-\pi/a}\right)}$	$\frac{e^{-\pi/a}(-1)^{k+1}+1}{2\pi(1-e^{-\pi/a})(1+k^2a^2)}$

2. MIMO NON-ISOTROPIC CHANNEL

In this section, we introduce our notations and assumptions for a MIMO wireless channel in a 2-dimensional (2D) non-isotropic random propagation media with omnidirectional antenna arrays. Throughout this paper superscripts B and M indicate variables at the BS and the MS sides.

Consider a moving MS with constant speed vector $\mathbf{v}(\frac{\mathrm{m}}{\mathrm{sec}})$ and a fixed BS. Antenna elements are located on the 2D azimuth plane at MS and BS sides around their local coordinates, O^B and O^M. We assume a propagation pattern for each antenna element denoted by $G_p^B(\theta^B;\omega)$ and $G_m^M(\theta^M;\omega)$ at frequency ω, for the p^{th} antenna at the BS and the m^{th} antenna at the MS, respectively, where $\theta^B \triangleq \angle\boldsymbol{\theta}^B$ and $\theta^M \triangleq \angle\boldsymbol{\theta}^M$. The unity vectors $\boldsymbol{\theta}^B$ and $\boldsymbol{\theta}^M$ represent a propagation direction (DOD or DOA) at BS and MS, respectively. Antenna elements are addressed by position vectors $\mathbf{a}_p^B$ and $\mathbf{a}_m^M$ versus local coordinates. We also assume that propagating waves are planar [5]. The inter-element scattering (the mutual coupling) is considered within the propagating patterns. We assume no line-of-sight since it can be separately considered.

By breaking down the received waveform into a linear combination of plane waves, we achieve a solution for Maxwell's equations. Each received waveform is associated with a path attenuation gain $g_{p,m;i}$, a path phase shift ϕ_i, a time-varying delay $\tau_{p,m;i}(t)$ and a complex gain composed of the antenna patterns at both BS and MS $G_p^B(\theta_i^B;\omega)G_m^M(\theta_i^M;\omega)$, where θ_i^B and θ_i^M are propagation directions associated with i^{th} path. The APP $G_p^B(\theta^B;\omega)$ and $G_m^M(\theta^M;\omega)$ are deterministic functions in terms of the propagation direction and the frequency. The STF channel TF between the p^{th} BS antenna and the m^{th} MS antenna is represented in terms of the carrier frequency as follows,

$$h_{mp}(t,\omega) = \tag{1}$$
$$= \sum_{i=1}^{I} G_p^B(\theta_i^B;\omega)G_m^M(\theta_i^M;\omega)g_{p,m;i}e^{(j\phi_i - j\varpi_i t - j\omega\tau_{p,m;i})},$$

where I is the number of dominant paths resulting from scattering, the Doppler shift $\varpi_i \triangleq \frac{\omega}{c}\mathbf{v}^T\boldsymbol{\theta}_i^M$ denotes the frequency shift of the signal along the i^{th} path caused by the Doppler effect, ω is the carrier frequency, and $\mathbf{v}$ and c are the MS velocity vector and the speed of light, respectively.

In this paper, we make the following statistical assumptions on the physical parameters:

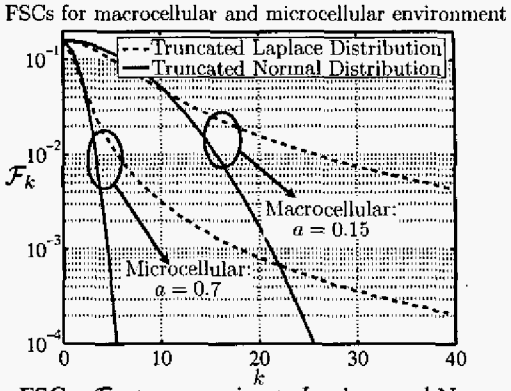

Fig. 1. FSCs, $\mathcal{F}_k$, to approximate Laplace and Normal distributions in different propagation environments; Macrocellular ($a = 0.15$rad) and Microcellular ($a = 0.7$rad).

A1) The pdf of the propagation directions, $f^B(\theta^B)$ and $f^M(\theta^M)$ over $[-\pi,\pi)$, characterize the non-isotropic propagation environment. Since these density functions are periodic with period of 2π, we can represent them by their FSE pairs as follows,

$$\mathcal{F}_k^B = \frac{1}{2\pi}\int_{-\pi}^{\pi} f^B(\theta)e^{-jk\theta}d\theta,\ f^B(\theta^B) = \sum_{k=-\infty}^{+\infty} \mathcal{F}_k^B\, e^{jk\theta^B},$$

$$\mathcal{F}_k^M = \frac{1}{2\pi}\int_{-\pi}^{\pi} f^M(\theta)e^{-jk\theta}d\theta,\ f^M(\theta^M) = \sum_{k=-\infty}^{+\infty} \mathcal{F}_k^M e^{jk\theta^M}.$$

Reported measurement results in literature [2–4, 6, 7] suggest two candidates for these pdfs namely truncated-Normal and truncated-Laplace distributions. Table 1 gives these distributions along with their FSCs, where $\mathrm{Re}\{.\}$ represents the real part of a complex variable, and $\mathrm{erf}(z) \triangleq \frac{2}{\sqrt{\pi}}\int_0^z e^{-u^2}du$ defines the Error function for a complex argument [8, Page 297]. Figure 1 compares the FSCs of these pdfs for two different macrocellular and microcellular situations; $a = 0.15$rad and $a = 0.7$rad, respectively. Let N_ϵ denotes the required number of FSCs in order to approximate the above pdfs with the required accuracy ϵ, such that $\forall k > N_\epsilon : |\mathcal{F}_k| < \epsilon$. Comparing the distributions in Figure 1, we see that the necessary number of FSCs for the Laplace pdf is $N_\epsilon = \frac{1}{a}\sqrt{\left(\frac{1+e^{-\frac{\pi}{a}}}{1+e^{-\frac{\pi}{a}}}\right)\frac{1}{2\pi\epsilon} - 1} \approx \frac{1}{a\sqrt{2\pi\epsilon}}$ larger than the necessary number of FSCs for the Normal pdf $N_\epsilon = \frac{1}{a}\sqrt{-2\ln(2\pi\epsilon)}$.

A2) The complex APPs, $G_p^B(\theta^B;\omega)$ and $G_m^M(\theta^M;\omega)$, give the response of antenna elements in terms of the propagation directions and the carrier frequency. These functions implicitly include the effect of the mutual coupling caused by the neighboring antenna elements [9, 10]. These pattern functions are all periodic functions of θ^B and θ^M with the period 2π. Therefore, we

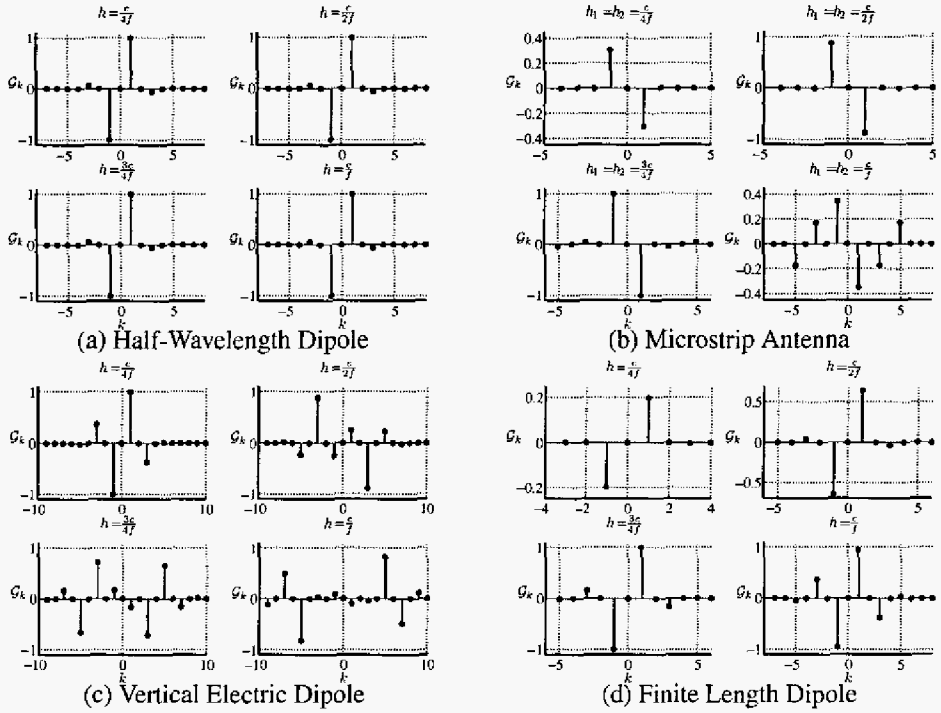

Fig. 2. Normalized Fourier Series Coefficients of Antenna Propagation Patterns, $\frac{\mathcal{G}_k}{\max_l |\mathcal{G}_l|}$ for four different commonly used antennas in wireless applications; (a) Half-Wavelength Dipole, (b) Microstrip Antenna, (c) Vertical Electric Dipole and (d) Finite Length Dipole. FSCs are presented for different antenna sizes; $h = h_1 = h_2 \in \left\{ \frac{c}{4f}, \frac{c}{2f}, \frac{3c}{4f}, \frac{c}{f} \right\}$.

represent them by their FSE as follows,

$$\mathcal{G}^B_{p,k} = \frac{1}{2\pi} \int_{-\pi}^{\pi} G^B_p e^{-jk\theta} d\theta, \;\; G^B_p = \sum_{k=-\infty}^{+\infty} \mathcal{G}^B_k e^{jk\theta^B},$$

$$\mathcal{G}^M_k = \frac{1}{2\pi} \int_{-\pi}^{\pi} G^M_p e^{-jk\theta} d\theta, \;\; G^M_p = \sum_{k=-\infty}^{+\infty} \mathcal{G}^M_k e^{jk\theta^M}.$$

where $G \triangleq G(\theta;\omega)$. Table 2 presents the APPs of some commonly used antennas. The half-wavelength dipole and microstrip antenna are often used for MIMO applications [9]. In this table, the parameters h, h_1 and h_2 are proportional with the size of the antenna and G_0 is the real constant and positive antenna gain that varies for each antenna. Figure 2 shows the FSCs of the underlined APPs when the carrier frequency is chosen to be $f = 2$GHz ($\omega = 2\pi f$), $h_1 = h_2 \triangleq h$ and $h \in \left\{ \frac{c}{4f}, \frac{c}{2f}, \frac{3c}{4f}, \frac{c}{f} \right\}$. We observe that, for all these antennas the value of $|\mathcal{G}_k|$ is considerable only for a limited number of coefficients. Also, we need more coefficients when the size of the antenna increases.

A3) The path phase shifts ϕ_is in (1) appear in the form of $e^{j\phi_i}$. The correlations of $e^{j\phi_i}$ over different paths, $E[e^{j(\phi_{i_1} - \phi_{i_2})}]$, have impact on the channel behavior. We assume that these correlations are non-zero only for similar paths. Specifically, we assume that the value of $E[e^{j(\phi_{i_1} - \phi_{i_2})}]$ is equal to κ^2 for similar paths and is zero for dissimilar paths where the number of similar paths for a specified path is limited by $I_{\text{sim}} < I$. The softness factor, $\kappa^2 \leqslant 1$, characterizes the effect of the environment on the phase correlation.

A4) We decompose the i^{th} path propagation delay, $\tau_{p,m;i}$, into three components in the following form:

$$\tau_{p,m;i} = \tau_i - (\tau^B_{p;i} + \tau^M_{m;i}), \tag{4a}$$

$$\tau^B_{p;i} \triangleq \frac{\mathbf{a}^{B^T}_p \boldsymbol{\theta}^B_i}{c}, \;\; \tau^M_{m;i} \triangleq \frac{\mathbf{a}^{M^T}_m \boldsymbol{\theta}^M_i}{c}, \tag{4b}$$

where τ_i represents the distance delay between O^B and O^M, and $\tau^B_{p;i}$ and $\tau^M_{m;i}$ represent relative propagation delays from antenna elements, $\mathbf{a}^B_p$ or $\mathbf{a}^M_m$, to corresponding coordinates, O^B or O^M. We assume i.i.d. Exponential distributions for time-delays, τ_i [11]. This distribution is defined as $\tau_i \sim \frac{1}{\sigma} e^{-\frac{\tau - \mu + \sigma}{\sigma}}$, $\forall \tau \geqslant \mu - \sigma$, where μ is the mean value to specify the distance between MS and BS and σ is the delay spread. The moment-generating-function (MGF) of the time-delay pdf is given by $\Phi_\tau(s) = \frac{e^{(\mu-\sigma)s}}{1-\sigma s}$.

Table 2. Antenna Propagation Patterns [9]

Antenna Type	APP, $G(\theta;\omega)$, $\forall\theta \in [-\pi,\pi)$
Half-Wavelength Dipole	$G_0 j\frac{\cos\left(\frac{\pi}{2}\cos\theta\right)}{\sin\theta}$
Microstrip Antenna	$-G_0 j\frac{\sin\left(\frac{\omega}{2c}h_1\sin\theta\right)\sin\left(\frac{\omega}{2c}h_2\cos\theta\right)}{\cos\theta}$
Vertical Electric Dipole	$G_0 j\sin\theta\left[2\cos\left(\frac{\omega}{c}h\cos\theta\right)\right]$
Finite Length Dipole	$G_0 j\frac{\cos\left(\frac{\omega}{2c}h\cos\theta\right)-\cos\left(\frac{\omega}{2c}h\right)}{\sin\theta}$

A5) When $|\tau_i| \gg \max\left\{|\tau^B_{p;i}|, |\tau^M_{m;i}|\right\}$, we formulate path-gain as a function of time-delay as:

$$g_{p,m;i} \simeq g_i = \sqrt{\frac{P_0}{I}}\tau_i^{-\frac{\eta}{2}}, \tag{5}$$

where η is the pathloss exponent ($\eta = 2$; free space propagation, $\eta = 4$; rural and $\eta = 6$; crowded urban environments [12]) and P_0 is a constant (see [5]).

3. CROSS-CORRELATION FUNCTION (CCF) FOR NON-ISOTROPIC PROPAGATION

Using above assumptions, we derive a closed-form expression for the STF-CCF between channel TFs of two arbitrary communication links, $h_{mp}(t_1,\omega_1)$ and $h_{nq}(t_2,\omega_2)$. This CCF is denoted by,

$$R_{mp,nq}(t_1,t_2;\omega_1,\omega_2) \triangleq E[h_{mp}(t_1,\omega_1)\, h^*_{nq}(t_2,\omega_2)], \tag{6}$$

and is a function of sampling times (t_1,t_2), carrier frequencies (ω_1,ω_2) and antenna elements $(m,p;n,q)$. By replacing (1) in (6), CCF $R_{mp,nq}(t_1,t_2;\omega_1,\omega_2)$ is written as,

$$E\Big[\sum_{i_1,i_2=1}^{I} G^B_p(\theta^B_{i_1};\omega_1)G^M_m(\theta^M_{i_1};\omega_1)g_{p,m;i_1}e^{-j\omega_1\tau_{p,m;i_1}(t_1)} \times e^{j(\phi_{i_1}-\phi_{i_2})}G^{B^*}_q(\theta^B_{i_2};\omega_2)G^{M^*}_n(\theta^M_{i_2};\omega_2)g_{q,n;i_2}e^{j\omega_2\tau_{q,n;i_2}(t_2)}\Big]. \tag{7}$$

By regrouping dependent and independent random variables in (7), replacing g_i from (5) and using Assumptions A1-A5, the expression of the CCF is decomposed as,

$$R_{mp,nq}(t_1,t_2;\omega_1,\omega_2) = \tag{8}$$
$$\frac{P_0}{I}\sum_{i_1,i_2=1}^{I}\Big\{E\left[(\tau_{i_1}\tau_{i_2})^{\frac{-\eta}{2}}e^{j\left(\omega_2\tau_{i_2}-\omega_1\tau_{i_1}\right)}\right]E\left[e^{j(\phi_{i_1}-\phi_{i_2})}\right]$$
$$\times E\left[G^B_p(\theta^B_{i_1};\omega_1)G^{B^*}_q(\theta^B_{i_2};\omega_2)e^{j\left(\frac{\omega_1}{c}\mathbf{a}_p^{B^T}\boldsymbol{\theta}^B_{i_1}-\frac{\omega_2}{c}\mathbf{a}_q^{B^T}\boldsymbol{\theta}^B_{i_2}\right)}\right]$$
$$\times E\Big[G^M_m(\theta^M_{i_1};\omega_1)G^{M^*}_n(\theta^M_{i_2};\omega_2)\times$$
$$e^{j\left(\frac{\omega_1}{c}\left(\mathbf{a}^M_m-\mathbf{v}t_1\right)^T\boldsymbol{\theta}^B_{i_1}-\frac{\omega_2}{c}\left(\mathbf{a}^M_n-\mathbf{v}t_2\right)^T\boldsymbol{\theta}^B_{i_2}\right)}\Big]\Big\}.$$

From Assumptions A4 and A5, the following expressions are derived for the first two expectations in (8),

$$E\left[(\tau_{i_1}\tau_{i_2})^{\frac{-\eta}{2}}\exp\left(j\left(\omega_2\tau_{i_2}-\omega_1\tau_{i_1}\right)\right)\right] =$$
$$= \begin{cases}\boldsymbol{\Phi}^{(\eta/2)}_\tau(j\omega_2)\,\boldsymbol{\Phi}^{(\eta/2)}_\tau(-j\omega_1), & i_1\neq i_2,\\ \boldsymbol{\Phi}^{(\eta)}_\tau(j(\omega_2-\omega_1)), & i_1=i_2,\end{cases} \tag{9}$$
$$E\left[\exp(j(\phi_{i_1}-\phi_{i_2}))\right] = \tag{10}$$
$$= \begin{cases}\kappa^2, & i_1\neq i_2 \;\&\text{ for two similar paths},\\ 0, & i_1\neq i_2 \;\&\text{ for two dissimilar paths},\\ 1, & i_1=i_2,\end{cases}$$

where $\boldsymbol{\Phi}_{\tau_i}(s) = \frac{e^{(\mu-\sigma)s}}{1-\sigma s}$ is the MGF of the time-delay, τ_i [5, Appendix I]. Calculating the last two expectation in (8), the CCF, $R_{mp,nq}(t_1,t_2;\omega_1,\omega_2)$, is formulated as follows,

$$P_0\boldsymbol{\Phi}^{(\eta)}_\tau(j(\omega_2-\omega_1))\mathcal{W}\left(\mathbf{d}^B_{p,q},\mathcal{G}^B_{p,k}(\omega_1)\otimes\mathcal{G}^{B^*}_{q,-k}(\omega_2)\otimes\mathcal{F}^B_k\right)$$
$$\times\ \mathcal{W}\left(\mathbf{d}^M_{m,n},\mathcal{G}^M_{m,k}(\omega_1)\otimes\mathcal{G}^{M^*}_{n,-k}(\omega_2)\otimes\mathcal{F}^M_k\right)+$$
$$+\ P_0 I_{\text{sim}}\kappa^2\boldsymbol{\Phi}^{(\frac{\eta}{2})}_\tau(-j\omega_1)\boldsymbol{\Phi}^{(\frac{\eta}{2})}_\tau(j\omega_2)\times \tag{11a}$$
$$\times\ \mathcal{W}\left(\mathbf{d}^B_p,\mathcal{G}^B_{p,k}(\omega_1)\otimes\mathcal{F}^B_k\right)\mathcal{W}\left(\mathbf{d}^B_q,\mathcal{G}^{B^*}_{q,-k}(\omega_2)\otimes\mathcal{F}^B_k\right)\times$$
$$\times\ \mathcal{W}\left(\mathbf{d}^M_m,\mathcal{G}^M_{m,k}(\omega_1)\otimes\mathcal{F}^M_k\right)\mathcal{W}\left(\mathbf{d}^M_n,\mathcal{G}^{M^*}_{n,-k}(\omega_2)\otimes\mathcal{F}^M_k\right),$$

$$\mathcal{W}\left(\mathbf{d},\mathcal{H}_k(\omega)\right) \triangleq 2\pi\sum_{k=-\infty}^{+\infty} j^k e^{jk\angle\mathbf{d}}\mathcal{H}_k(\omega)J_k\left(\frac{|\mathbf{d}|}{c}\right), \tag{11b}$$

$$\mathbf{d}^B_{p,q} \triangleq \omega_1\mathbf{a}^B_p-\omega_2\mathbf{a}^B_q, \tag{11c}$$

$$\mathbf{d}^M_{m,n} \triangleq (\omega_2 t_2-\omega_1 t_1)\,\mathbf{v}+\left(\omega_1\mathbf{a}^M_m-\omega_2\mathbf{a}^M_n\right), \tag{11d}$$

$$\mathbf{d}^B_p \triangleq \omega_1\mathbf{a}^B_p,\ \mathbf{d}^B_q \triangleq \omega_2\mathbf{a}^B_q, \tag{11e}$$

$$\mathbf{d}^M_m \triangleq \omega_1(\mathbf{a}^M_m-t_1\mathbf{v}),\ \mathbf{d}^M_n \triangleq \omega_2(\mathbf{a}^M_n-t_2\mathbf{v}), \tag{11f}$$

$\mathcal{G}_k(\omega)$ and $\mathcal{F}_k$ are the FSEs of the APP and the AAS in the corresponding coordinates, respectively, $J_k(z) \triangleq \frac{j^{-k}}{\pi}\int_0^\pi e^{j(ku+z\cos u)}du$ is the k^{th}-order Bessel function of the first kind, and $\otimes$ and $|.|$ denote the convolution and the Euclidian norm, respectively. In Assumption A4, we consider Exponential distribution for the delay profile (DP). By integrating the MGF, $\boldsymbol{\Phi}_\tau(s)$, η^{th}-times, we obtain the expression of $\boldsymbol{\Phi}^{(\eta)}_\tau(s)$ as given in [5]. We call the vectors $\mathbf{d}^B_{(..)}$ and $\mathbf{d}^M_{(...)}$ as the separation vectors. These separation vectors illustrate the impact of the location of antennas, the time indices and the carrier frequencies and the mobile speed at BS and MS on the CCF, respectively. The norm of these vectors (divided by c) are the arguments of the Bessel functions. Therefore, these norms represent a combination of the spatial, the temporal and the frequency separations between $h_{mp}(t_1,\omega_1)$ and $h_{nq}(t_2,\omega_2)$.

In [13] we present the Fourier analysis of the derived CCF for a narrowband communication system $\omega_1 = \omega_2 = \omega$,

when $\kappa = 0$ and we employ one antenna in the MS side. Figure 3 shows the impact of non-isotropic propagation and non-omnidirectional antenna in comparison with isotropic propagation with omnidirectional antenna. The results are shown for $a = 0.44$.

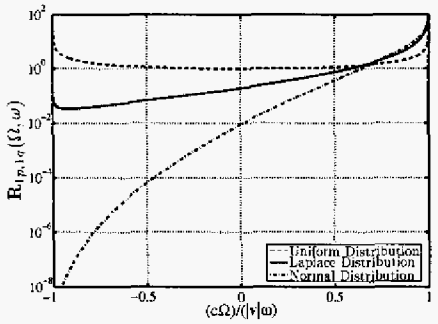

(a) Omnidirectional Antenna

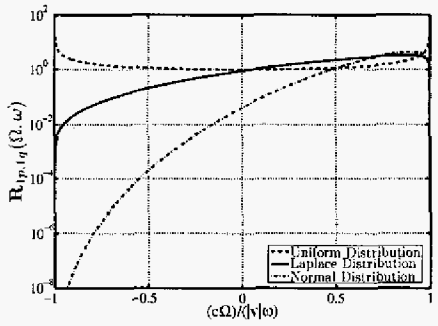

(b) Half-Wavelength Dipole

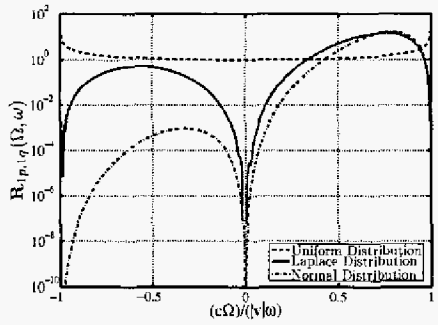

(c) Microstrip Antenna

Fig. 3. Normalized Power Spectral Density (PSD) for Stationary CCF and moving MS on the positive direction of the x-axis: (a) Omnidirectional antenna, (b) Half-Wavelength Dipole and (c) Microstrip Antenna.

4. CONCLUSIONS

The non-isotropic scattering introduces a linear combination of Bessel functions of different orders to represent the spatial-temporal-frequency selectivities of the CCF. The weights of Bessel functions come from FSCs of the AAS and FSCs of the APP. We also show impacts of non-isotropic environment and non-omnidirectional antennas on the spectrum of the received channel process while the maximum Doppler frequency shift remains invariant with variations of beam-patterns and the pdf of propagating waves.

5. REFERENCES

[1] G. Durgin, *Space-Time Wireless Channels*. NJ: Prentice Hall, 2003.

[2] U. Martin, "Spatio-temporal radio channel characteristics in urban macrocells," *IEE Proceedings - Radar, Sonar and Navigation*, vol. 45, pp. 42–49, Feb. 1998.

[3] K. I. Pedersen, P. E. Mogensen, and B. H. Fleury, "A stochastic model of the temporal and azimuthal dispersion seen at the base station in outdoor propagation environments," *IEEE Transactions on Vehicular Technology*, vol. 49, pp. 437–447, March 2000.

[4] A. Abdi, J. A. Barger, and M. Kaveh, "A parametric model for the distribution of the angle of arrival and the associated correlation function and power spectrum at the mobile station," *IEEE Transactions on Vehicular Technology*, vol. 51, pp. 425–434, May 2002.

[5] S. Gazor and H. S. Rad, "Delay-frequency characterization of mimo wireless channels," *IEEE Transactions on Wireless Communications*, to appear, 2005.

[6] S. A. Zekavat and C. R. Nassar, "Power-azimuth-spectrum modeling for antenna array systems: a geometric-based approach," *IEEE Transactions on Antennas and Propagation*, vol. 51, pp. 3292–3294, Dec. 2003.

[7] A. Tang and K. Gong, "Study on power azimuth spectrum of wireless channel in microcell environments," in *IEEE Proceedings on Personal, Indoor and Mobile Radio Communications, (PIMRC'03)*, 14, Sept. 2003.

[8] M. Abramowitz and I. A. Stegun, *Handbook of Mathematical Functions with Formulas, Graphs, and Mathematical Table*. NY: Dover Publications INC., June 1974.

[9] C. A. Balanis, *Antenna Theory: Analysis and Design*. John Wiley & Sons, 2 ed., 1996.

[10] M. K. Ozdemir, H. Arslan, and E. Arvas, "On the correlation analysis of antennas in adaptive mimo systems with 3-d multipath scattering," in *IEEE Wireless Communications and Networking Conference, (WCNC'04)*, March 2004.

[11] W. C. Jakes, *Microware Mobile Communications*. New York: Wiley, 1974.

[12] T. Rappaport, *Wireless Communications - Principles and Practice*. Prentice Hall PTR, 1996.

[13] H. S. Rad and S. Gazor, "The impact of non-isotropic scattering and non-omnidirectional antennas on mimo communication channels," *IEEE Transactions on Antenna and Propagation*, submitted, 2005.